

A11102 616328

NAT'L INST OF STANDARDS & TECH R.I.C.



A11102616328

Mulholland, George W/Simulation of aeros
QC100 .U56 NO.86-3342 1986 V19 C.1 NBS-P

NB

Simulation of Aerosol Agglomeration in the Free Molecular and Continuum Flow Regimes

George W. Mulholland
Raymond D. Mountain
Howard Baum

U.S. DEPARTMENT OF COMMERCE
National Bureau of Standards
National Engineering Laboratory
Center for Fire Research
Gaithersburg, MD 20899

March 1986

Prepared for:
Defense Nuclear Agency
Department of Defense
Washington, DC 20305

QC

100

.U56

#86-3342

1986

c.2

NEBC
00107
006
NO 2-34
1986
3-7

NBSIR 86-3342

**SIMULATION OF AEROSOL
AGGLOMERATION IN THE FREE
MOLECULAR AND CONTINUUM FLOW
REGIMES**

George W. Mulholland
Raymond D. Mountain
Howard Baum

U.S. DEPARTMENT OF COMMERCE
National Bureau of Standards
National Engineering Laboratory
Center for Fire Research
Gaithersburg, MD 20899

March 1986

Prepared for:
Defense Nuclear Agency
Department of Defense
Washington, DC 20305



U.S. DEPARTMENT OF COMMERCE, Malcolm Baldrige, *Secretary*
NATIONAL BUREAU OF STANDARDS, Ernest Ambler, *Director*

TABLE OF CONTENTS

	<u>Page</u>
List of Figures	iv
Abstract	1
1. INTRODUCTION	2
2. COMPUTATIONAL TECHNIQUE	4
3. FRICTION FORCE	8
3.1 Free Molecular Regime	8
3.2 Continuum Regime	10
4. RESULTS	20
4.1 Structure	20
4.2 Kinetics	25
4.3 Cluster Size Distribution	30
5. COAGULATION EQUATION	35
6. COMPARISON WITH EXPERIMENTS	41
7. ACKNOWLEDGMENT	42
8. REFERENCES	43

LIST OF FIGURES

	<u>Page</u>
Figure 1. Planar projection of an agglomerate with 90 spheres	21
Figure 2. R_g^2 vs k for $\beta\tau = 0.05$ and $\rho = 0.0167$	22
Figure 3. R_g^2 vs k for continuum flow for $\rho = 0.0167$	24
Figure 4. Reduced number concentration versus time steps for free molecular flow	26
Figure 5. Reduced number concentration versus reduced time for $\beta\tau = 0.05$	28
Figure 6. Reduced number concentration versus t_N for continuum flow	29
Figure 7. The cluster size distribution is plotted for free molecular simulation for $N_0/N(t) = 4.5$	31
Figure 8. The cluster size distribution is plotted for $N_0/N(t) = 8.7$ for the same simulation as Figure 7	32
Figure 9. The cluster size distribution is plotted for the continuum simulation for $N_0/N(t) = 3$	33
Figure 10. The cluster size distribution is plotted for $N_0/N(t) = 9$ for the same simulation as Figure 9	34

SIMULATION OF AEROSOL AGGLOMERATION IN THE FREE
MOLECULAR AND CONTINUUM FLOW REGIMES

George W. Mulholland, Raymond D. Mountain and Howard Baum

Abstract

The formation of high temperature aerosol agglomerates is simulated by following the Langevin trajectory of each particle with the boundary condition that the particles stick upon collision. Both the free molecular and continuum flow are treated. A new derivation of the friction force of an agglomerate in the continuum limit is developed based on the evaluation of the surface momentum flux at the Oseen flow limit. The agglomerates can be described as a fractal, at least in regard to power law relationship between mass and size, with a dimensionality of 1.7-1.9 independent of the flow regime. The particle growth is shown to be much more rapid in the free molecular regime than in the continuum. The global kinetics are shown to be consistent with a similarity analysis of the coagulation equation with a modified coagulation coefficient. Comparison between the simulation and coagulation theory at small time suggests a slight fluctuation enhancement in the free molecule case and a small-time enhancement of the coagulation rate at high concentration for the continuum case.

Keywords: aerosol agglomeration, agglomerates, Brownian motion, Darcy's law, fractal dimension, free molecular regime, Smoluchowski equation, soot.

1. INTRODUCTION

Aerosol agglomerates are formed in high temperature processes including soot formed in flames and in engines, silica produced through the combustion of silane, and metal particles produced by vaporization of a metal as a result of joule heating. This last method is known as the exploding wire technique [1] for aerosol production. The particle growth processes include nucleation, surface growth (or condensation), and coagulation. Initially the particles may coalesce upon colliding and sticking, but eventually the particles retain their structure upon collision and a cluster made up of individual spherules evolves. It is the latter cluster growth process that is the subject of this paper.

One of the first models of cluster growth was developed by Sutherland [2] for studying floc structures in colloids. Cluster growth in this model is treated geometrically as a series of random collisions between particles and particle clusters. Meakin [3] and Kolb et al. [4] have developed cluster-cluster aggregation models based on random walk motion of the clusters. The diffusion coefficient of the cluster is assumed to have a power law dependence on the number of spheres in the cluster.

In three dimensions the structures found in these models are quite open and the degree of openness has been characterized in terms of a fractal dimensionality, D , which can be defined by the following equation:

$$m \sim r^D.$$

The quantity m represents the mass of the object and r its radius. For a solid three-dimensional object, $D=3$. Meakin [3] has obtained $D \approx 1.8$ for agglomerates. The fact that the dimensionality is less than three implies that the average density decreases with increasing radius.

We use the term agglomeration to refer to the growth process in which clusters collide and stick together. Our usage of the term agglomeration is essentially identical with Meakin's cluster-cluster aggregation terminology. This differs from the model originally developed by Vold [5] in which individual particles are added one at a time to a growing cluster. The Vold-like growth process we term aggregation. Witten and Sander [6] have developed a diffusion limited aggregation model in which the individual particles are added one at a time via Brownian motion to a stationary aggregate. Richter et al. [7] have used this model for describing soot growth and obtain a more dense structure than is obtained with the agglomeration models. The Richter et al. structure has a fractal dimension of about 2.4.

Our simulation differs from the others in that we follow the trajectory of every cluster. This enables straightforward comparison with the kinetics of a real system. The so-called Brownian dynamics method that we use places a premium on the use of an efficient computer code because of the complex structures that develop. The general procedure for carrying out the simulation is described in the next section, while the architecture of the computer code is described in a second paper [8].

A necessary input to the simulation is the friction force acting on the agglomerate. In section 3 we derive expressions for the friction force in the

free molecular limit, which is approached at flame conditions, and in the continuum limit, which becomes more valid as large agglomerates are formed in a rising smoke plume. Our continuum result is compared with the results obtained by Meakin et al. [9] based on the Kirkwood-Riseman theory.

One of the principal results of our study is the characterization of the agglomerate structure with a fractal dimension. The results of this simulation are compared with Meakin's results [3] based on random walk of the clusters on a lattice. The second area of major interest is the global kinetics of the agglomeration process. The results from the simulation are compared with a prediction based on a similarity solution of the coagulation equations in section 5. The results are also compared with available experimental results on the structure of the agglomerate and kinetics in section 6.

2. COMPUTATIONAL TECHNIQUE

This simulation is based on the assumption that the agglomerating particles move subject to the rules of Brownian motion plus the condition that if two agglomerates "touch", as defined below, they stick and the resulting agglomerate also rigidly diffuses according to the Brownian motion rule. The "rule" for Brownian motion is that the dynamics of a particle are governed by the Langevin equation

$$d(mv_x)/dt = -m\beta v_x + f_x \quad (1)$$

where v_x is the xth cartesian component of the velocity of the center of mass of the agglomerate of mass m and f_x is a stochastic force satisfying

$\langle f_x^2 \rangle = 2\beta m k_o T$. As can be seen from eq. (1), β^{-1} represents the relaxation time of the agglomerate. The quantity β is the controlling parameter for the dynamics. In addition, the center of mass of the aggregate moves according to

$$dx/dt = v_x, \quad (2)$$

subject to periodic boundary conditions. In the work reported here, we have used the Ermack and Buckholtz [10] solution of the Langevin equations given by

$$\vec{r} = \vec{r}_o + \frac{1}{\beta} (\vec{v} + \vec{v}_o) \tanh (\beta h/2) + \vec{B}_2 \quad (3)$$

and

$$\vec{v} = \vec{v}_o e^{-\beta h} + \vec{B}_1 \quad (4)$$

for the positions, $\{\vec{r}\}$, and velocities, $\{\vec{v}\}$, at time $t+h$ given positions $\{\vec{r}_o\}$ and velocities $\{\vec{v}_o\}$ at time t . The stochastic integrals \vec{B}_1 and \vec{B}_2 satisfy

$$\langle \vec{B}_1 \rangle = \langle \vec{B}_2 \rangle = \langle \vec{B}_1 \cdot \vec{B}_2 \rangle = 0, \quad (5)$$

$$\langle B_1^2 \rangle = 3 \frac{k_B T}{m} [1 - \exp (-2\beta h)], \quad (6)$$

and

$$\langle B_2^2 \rangle = \frac{6 k_B T}{m\beta^2} [\beta h - 2 \tanh (\beta h/2)]. \quad (7)$$

This solution assumes that the diffusing particles are in thermal equilibrium with the background gas through which they move. It should be noted that this solution is contained in the 1943 Reviews of Modern Physics article by Chandresakhar [11]. The development in this article is also an important advance in the application of stochastic methods to random processes in condensed matter physics.

Initially, we used a program which was a straightforward adaptation of the molecular dynamics codes which had been used by Mountain [12] in other studies. As a result of lessons learned by applying some of the techniques developed in computer science to the molecular dynamics problem [13], we attempted to apply these techniques to the agglomeration problem. The result was a reduction by a factor of 4 in the execution time of the simulation program. A detailed description of the efficient, scalar program is described in a second paper [8]. The basic idea implemented in this program is that particles which are within unit distance of other particles "touch" and are therefore within the same cluster and are identified as such. Then list manipulation techniques are used to implement the sticking conditions and to identify the newly formed clusters in updated lists.

It is our practice to generate ten sets of initial conditions so that adequate averaging is possible. The initial conditions consist of a set of coordinates for 500 spheres of mass m_0 and unit diameter σ . The coordinates are generated by a uniform random number generator which places the initial positions of the particles in a cube of side L . The initial velocities are obtained using a random number generator which produces normally distributed numbers with unit variance so that the particles are in thermal equilibrium

with the background gas through which they diffuse. In this way, the temperature, T , and hence the energy unit, $k_B T$, for the simulation, is specified. The unit of time $\tau = (m_o \sigma^2 / k_B T)^{1/2}$ is the time required for a single sphere to freely stream a distance equal to its diameter σ . The particles move according to equations (3) and (4) for a time interval h . Periodic boundary conditions are used to eliminate the influence of the surface of the cube of side L on the motion of the agglomerates. After each interval h , the system is examined to see if any agglomeration events have occurred. If a new agglomeration event has occurred, the lists containing cluster information are updated and the size and the radius of gyration of the existing clusters are determined. This process is repeated until a specified number of iterations of the equations of motion have been made. As noted above, averages over ten sets of initial conditions are made. This results in good statistics for the smaller clusters but relatively poor statistics for the few larger clusters generated.

It should be noted that the clusters are only allowed to translate. In principle the clusters should also be allowed to rotate, subject to a rotational Brownian motion rule. We intend to examine this topic in a future study. Meakin [14] has shown for a two-dimensional model that rotation in "equilibrium" with translation does not significantly change the fractal dimensionality of the resulting clusters.

3. FRICTION FORCE

3.1 Free Molecular Regime

Soot particles in flames approach free molecular conditions because of both the small particle size ($\sim 0.02 \mu\text{m}$) and the increased mean free path of the gas ($0.2 - 0.3 \mu\text{m}$) at the flame temperature. In this limit, Epstein [15] showed that the friction coefficient for a sphere, K , is proportional to the particle cross section, πR^2 , and to the average thermal speed, \bar{v} , of the host gas molecules.

$$K = m_o \beta = \frac{4}{3} \delta \pi R^2 \frac{P}{k_B T} m_g \bar{v} \quad (8)$$

The quantity m_g refers to the mass of a gas molecule, P to the gas pressure, and δ to the surface accommodation factor which has a value of 1 for specular reflection and a value of 1.444 for diffuse reflection.

We approximate the friction coefficient of a cluster made up of k spheres as k times the friction coefficient of a single sphere. In making this approximation we neglect the shielding effect of the other spheres, but for a tenuous, low density agglomerate this is a reasonable first approximation. In any event, it is an approximation that will ultimately require testing.

As pointed out earlier in the paper, the quantity β^{-1} , which appears in eq. (1), corresponds to the relaxation time of the agglomerate. The apparent agglomerate mean free path, λ_p , is obtained from $\bar{v}_p \beta^{-1}$, where \bar{v}_p refers to the average thermal speed of the particle. If λ_p is large compared to the

particle diameter, the particle behavior is free molecular. Equivalently, the free molecular condition corresponds to the relaxation time, β^{-1} , being long compared to the time, τ , to free stream a particle diameter; that is,

$$\beta\tau \ll 1. \quad (9)$$

From the definition of τ and from eq. (8), we obtain the following result in the free molecular limit:

$$\beta\tau = \frac{4\sqrt{2}}{\rho_s k_B T} \frac{\delta P}{\sqrt{m_o m_g}}, \quad (10)$$

where m_o is the mass of an individual sphere, ρ_s refers to its density, and m_g the mass of the gas molecules. Our simulations are carried out for $\beta\tau = 0.2$, which corresponds to an 8 nm particle radius for a 1500 K flame temperature, and for $\beta\tau = 0.05$, which corresponds to a 3 nm radius. The density of the individual particles is taken to be 2.0 g/cm^3 and ambient pressure is assumed.

In the simulation it is assumed that when two particles collide and stick together, the new aggregate moves with the thermally accommodated velocity. The average interparticle spacing at the start of the simulation is in the range 2.7 particle diameters to 5.8 particle diameters. In an actual aerosol, the interparticle spacing is much greater, on the order of 100 or greater. This greater spacing provides time for thermal accommodation with the host gas before a newly formed agglomerate collides with another agglomerate. An estimate of the momentum relaxation time can be obtained by integrating the Langevin equation, eq. (1), to obtain the root mean particle velocity $\langle v_x^2(t) \rangle^{1/2}$, assuming the particle is initially at rest.

$$\langle v_x^2(t) \rangle^{1/2} = \sqrt{\frac{k_B T}{m}} (1 - e^{-2\beta t})^{1/2} \quad (11)$$

The time, t_m , at which $\langle v_x^2(t) \rangle^{1/2}$ increased to $(1 - e^{-1})$ of its final value is given by

$$t_m = \frac{0.255}{\beta} . \quad (12)$$

The corresponding free streaming distance traveled would be 1.3 and 5.1 particle diameters for $\beta\tau$ equal to 0.2 and 0.05, respectively. So it is seen that thermal accommodation may not occur at the high concentration, low $\beta\tau$ case, before a second collision occurs in the simulation. To avoid this non-physical effect, the agglomerates are thermally accommodated after each collision in the simulation.

3.2 Continuum Regime

As the soot particles grow to a size approaching a micrometer in diameter in the near ambient conditions of the rising smoke plume, the continuum limit may become a more valid description for the friction force because of the increased particle size and decreased mean free path. Continuum flow is valid in the limit of the characteristic length scale of the structure being much greater than the mean free path of the gas. We first derive a general expression for the friction force in the continuum limit in terms of a surface integral involving the stress tensor and momentum flux. The flow field is derived based on Stokes flow in the vicinity of the agglomerate and Oseen flow far from the agglomerate. The solution technique is similar to the matched asymptotic expansion applied by Proudman and Pearson [16] to a solid sphere.

The technique is also described by Van Dyke [17]. In our case we have a porous agglomerate rather than a solid sphere. We treat the agglomerate as a porous medium obeying Darcy's law in regard to flow within the agglomerate. Felderhof [18] has treated an analogous problem of the friction coefficient of a polymer by a technique that apparently does not involve Oseen flow.

Because previous analyses have not included the convective term, we present a consistent hydrodynamic analysis of the friction force including the convective term even though the result is similar to that of the previous analyses [18]. For the reader interested in the final expression for the friction force used in the simulations, he may go directly to eq. (45) without loss of continuity.

We begin our analysis with the equation for the momentum flux for an incompressible fluid with density ρ .

$$\frac{\partial}{\partial t} (\rho v_i) = - \frac{\partial p}{\partial x_i} - \frac{\partial}{\partial x_k} (\rho v_i v_k) + \eta \frac{\partial^2 v_i}{\partial x_k \partial x_k} \quad (13)$$

We consider steady state flow for which the time derivative in eq. (13) vanishes. To obtain the friction force, we first integrate the right hand side over the entire fluid volume contained between the complex agglomerate surface, s_a , and the outer surface, s_o , of radius r_o . Then using the divergence theorem, we obtain

$$\oint_{s_o} \rho v_i v_k n_k dA - \oint_{s_a} \rho v_i v_k n_k dA = \oint_{s_o} \sigma_{ik} n_k dA - \oint_{s_a} \sigma_{ik} n_k dA, \quad (14)$$

where n_k refers to the outward normal to the surface and where

$$\sigma_{ik} = -p\delta_{ik} + \sigma_{ik} = -p\delta_{ik} + \eta \left(\frac{\partial v_i}{\partial x_k} + \frac{\partial v_k}{\partial x_i} \right) \quad (15)$$

At the surface of the agglomerate, the fluid velocity vanishes so the second term on the LHS of eq. (14) vanishes. The second term on the RHS of eq. (14) corresponds to the force on the particle; that is, to the friction force, F_i , that we wish to calculate.

$$F_i = \oint_{sa} \sigma_{ik} n_k dA \quad (16)$$

Thus we obtain the following general result for the friction force of an agglomerate of arbitrary shape in terms of a surface integral.

$$F_i = \oint_{so} [\sigma_{ik} - \rho v_i v_k] n_k dA \quad (17)$$

To solve for F_i we must determine the pressure and velocity for large r . For incompressible flow, the steady state Navier-Stokes equation can be written as

$$\rho (\vec{v} \cdot \nabla) \vec{v} + \nabla p - \eta \Delta \vec{v} = 0 \quad (18)$$

with

$$\nabla \cdot \vec{v} = 0. \quad (19)$$

First we consider the behavior close to the agglomerate for which the Reynolds number, ϵ , is small and the convective term may be neglected. Taking the divergence of eq. (18) and making use of eq. (19), we obtain

$$\nabla^2 p = 0 \quad (20)$$

A trial solution for p in terms of spherical coordinates is given by

$$p = p_0 - v_0 \eta \cos\theta \chi(r). \quad (21)$$

Substituting from eq. (21) into eq. (20), we find

$$r^2 \chi'' + 2 r \chi' - 2 \chi = 0. \quad (22)$$

The solution to eq. (22) remaining finite as $r \rightarrow \infty$ is given by

$$\chi = \frac{A}{r} \quad r > R, \quad (23)$$

where R is the radius of the agglomerate.

We chose the fluid velocity far from the agglomerate to be v_0 in the z direction. It is convenient to use Felderhof's [18] suggested form for \vec{v} in spherical coordinates.

$$\vec{v}(r) = v_0 \left\{ \phi(r) \cos\theta e_r - \left[\phi(r) + \frac{1}{2} r \phi'(r) \right] \sin\theta e_\theta \right\} \quad (24)$$

This form insures that $\nabla \cdot \vec{v}(r) = 0$. Substituting from eqs. (24) and (21) for \vec{v} and p into eq. (18) with the convective term dropped, we find

$$r^2 \phi''(r) + 4r \phi'(r) + r^2 \chi'(r) = 0 \quad (25)$$

Substituting from eq. (23) for χ and solving the differential equation, we obtain

$$\phi = 1 - \frac{A}{r} + \frac{B}{r^3} \quad r > R \quad (26)$$

Far from the body such that $\epsilon r/R$ is of order unity, the first term in eq. (18), the convective term, can not be neglected. It is convenient to use the following reduced variables

$$\begin{aligned} \vec{v}' &= \vec{v}/v_0 \\ p &= p_0 + \frac{v_0 R}{\eta} p' \end{aligned} \quad (27)$$

$$x'_i = \epsilon x_i / R$$

Since there is no longer spherical symmetry with the convective term included, the equations will be expressed in terms of cartesian coordinates. From eqs. (23) and (26), we obtain v'_i to order ϵ for the Stokes solution.

$$v'_i = \delta_{i3} + \epsilon \left[-\frac{A\delta_{i3}}{2Rr'} - \frac{1}{2} \frac{Ax'_i x'_3}{Rr'^3} \right] \quad (28)$$

The lowest order term in the pressure equation is given by

$$p' = \frac{\epsilon^2 Ax'_3}{Rr'^3} \quad (29)$$

The form of the solution of the Stokes problem suggests the following expansion for v' and p' for the solution of the Navier-Stokes equation to leading order

$$v'_i = \delta_{i3} + \varepsilon \tilde{v}_i(x'_k) \quad (30)$$

$$p' = \varepsilon^2 \tilde{p}(x'_k) \quad (31)$$

Substituting eqs. (30) and (31) into eqs. (18) and (19), we obtain to lowest order

$$\frac{\partial \tilde{v}_i}{\partial x'_3} + \frac{\partial \tilde{p}}{\partial x'_i} = \Delta \tilde{v}_i \quad (32)$$

$$\frac{\partial \tilde{v}_i}{\partial x'_i} = 0 \quad (33)$$

This version of the Oseen flow problem was analyzed by Lamb [19]. The solution is

$$\tilde{v}_i = \frac{Ax'_i}{Rr'} - \frac{A}{2R} e^{(x'_3 - r')/2} \left[\frac{\delta_{i3}}{r'} + \frac{x'_i}{r'} \left(\frac{2}{r'^2} + \frac{1}{r'} \right) \right] \quad (34)$$

By expanding the exponential term in eq. (34) for the limit of small r' corresponding to small Reynolds number, ε , one finds that eq. (34) is consistent with the Stokes solution given in eq. (28). We note that taking the divergence of eq. (18) still results in a harmonic equation for the pressure. So eq. (29) is still valid for the pressure.

The convective component of the friction force is given by

$$F_i = - \rho \oint v_i v_k n_k dA \quad (35)$$

Substituting from eqs. (30) and (34) into eq. (35) and expanding, we obtain

$$\begin{aligned}
F_i = & -\rho v_o^2 \delta_{i3} \delta_{k3} \oint n_k dA - \rho v_o^2 \delta_{i3} \epsilon \oint \tilde{v}_k n_k dA \\
& - \rho v_o^2 \delta_{k3} \epsilon \oint \tilde{v}_i n_3 dA - \rho v_o^2 \epsilon^2 \oint \tilde{v}_i \tilde{v}_k n_k dA
\end{aligned} \tag{36}$$

The first term vanishes by symmetry, the second term vanishes since fluid is incompressible, and the last term vanishes as $1/r_o$. Substituting for \tilde{v}_i from eq. (34) and carrying out the integration in cylindrical coordinates suggested by the cylindrically symmetric wake structure, we obtain

$$F_3 = F_z = 4\pi A v_o \eta \tag{37}$$

$$F_x = F_y = 0$$

We find that the stress tensor component of F_3 vanishes in the limit of large r_o , so eq. (37) gives the total contribution to the friction force.

We point out that Felderhof's result [18] is essentially identical to eq. (37), however, in his case the entire contribution is from the stress tensor term. He does not include the convective term found in eq. (18) even for the integration over all space. It is a surprising coincidence that the two expressions are identical.

To determine the coefficient A, we model the flow inside the agglomerate as flow through a porous object satisfying Darcy's law.

$$\nabla p + \frac{\eta}{\kappa} \vec{v} = 0 \tag{38}$$

The quantity κ is the hydrodynamic permeability. Again we assume the fluid to be incompressible and find the following results for χ and ϕ within the porous sphere.

$$\chi = Cr \quad r < R \quad (39)$$

$$\phi = C\kappa \quad r < R \quad (40)$$

The coefficient A appearing in eq. (37) is obtained by requiring continuity of pressure and of radial and angular velocity at the surface of the porous sphere. We obtain

$$A = \frac{R}{2/3 + \kappa/R^2} \cdot \quad (41)$$

So from eq. (37) we obtain the following expression for the friction force:

$$F_z = \frac{6\pi R v_o \eta}{1 + \frac{3}{2} \frac{\kappa}{R^2}} \quad (42)$$

In the impermeable sphere limit $\kappa/R^2 \rightarrow 0$ the Stokes formula for the friction force is recovered. For the case where $\kappa/R^2 \gg 1$, called the free draining limit for polymers, we find

$$F_z = \frac{4}{3} \pi \eta R^3 v_o / \kappa. \quad (43)$$

There are not adequate experimental data to determine which of these limits is more nearly appropriate for aerosol agglomerates. We suspect that the limit $\kappa/R^2 \rightarrow 0$ to be the correct limit for the reasons discussed below.

Assuming κ to be inversely proportional to the agglomerate density and taking R to be the radius of gyration of the agglomerate, we find that

$$\frac{\kappa}{R_g^2} \sim R_g^{D-1}$$

So provided that the fractal dimension $D > 1$, which is the case as we show below for agglomerate growth, then the term $\frac{3}{2} \kappa/R_g^2$ can be neglected for large R_g . Felderhof and Deutch [20] derived an inverse density dependence for κ in the related problem of the friction coefficient for polymers. In our simulations, lacking specific information on κ , we drop the second term in the denominator and use the expression,

$$K = m\beta = 6\pi\eta R_g. \quad (44)$$

This Stokes-Einstein type expression suggests that the fluid is trapped in the agglomerate and that the entire assembly moves as if it were a compact sphere of radius R_g .

For the simulations carried out in this study, we assume the primary sphere has a radius of $0.5 \mu\text{m}$, $\rho_s = 2$, and $T = 298 \text{ K}$ at ambient pressure. From eq. (44) and the definition of τ , we obtain the following:

$$\beta\tau = 6 \eta R_g \left(\frac{6\pi}{\rho_s \sigma k_B T} \right)^{1/2} = 84 \quad \text{single sphere} \quad (45)$$

$$\beta\tau = \frac{6\eta R_g}{k} \left(\frac{6\pi}{\rho_s \sigma k_B T} \right)^{1/2} = \frac{167 (R_g/\sigma)}{k} \quad \text{agglomerate} \quad (46)$$

$$\beta\tau = 55 \quad \text{doublet} \quad (47)$$

The quantities σ refers to the primary particle diameter and R_g the radius of gyration. The value of $\beta\tau$ for the doublet was taken to be the orientation averaged value of a spheroid with major axis 2σ and minor axis σ [21]. This value agrees within 10% with the measured friction coefficient based on a sedimentation experiment [22]. For agglomerates with three or more spheres, equation (46) is used.

Meakin et al. [9] have calculated the friction force in the continuum limit based on the Kirkwood-Riseman theory [23]. The hydrodynamic interactions in this theory are the far field limits where a particle is treated as a force field from a point in regard to its effect on other particles. For a specified configuration of spheres in the cluster, the friction coefficient was calculated and expressed in the form

$$K = 6\pi\eta R_h,$$

where R_h is the hydrodynamic radius. Calculations were performed for agglomerates with 50 to 350 particles. The quantity R_h was fitted to a power law relationship of the form $R_h \sim k^\gamma$, where k refers to the number of spheres in the agglomerate and the exponent γ has a value of 0.544 ± 0.014 . The radius of gyration, R_g , was also found to have a power law relationship of the form $R_g \sim k^\alpha$ with exponent α , 0.554 ± 0.038 , within the error limits of the exponent γ . So we see that R_g and R_h have a similar dependence on k and consequently the expressions for k obtained by our macroscopic hydrodynamic description of the flow, eq. (44), and obtained by the detailed flow field analysis by Meakin et al. are similar. There are no data available to test the theories.

The values of $\beta\tau$ are obviously much greater in the continuum than in the free molecular limit. In the continuum, the agglomerate diffuses only a small fraction of a particle diameter before its direction of motion is significantly changed whereas the free molecular particles move several particle diameters before changing their direction. Also in the free molecular case $\beta\tau$ is independent of the number of spheres in the agglomerate k , while $\beta\tau$ decreases with increasing k in the continuum limit.

4. RESULTS

4.1 Structure

The structure of the agglomerate is quite open as indicated in Fig. 1 for a planar projection of the structure. This particular simulation is for the free molecular limit with $\beta\tau = 0.2$, but similar structures are also obtained in the continuum limit. A quantitative measure of the structure is obtained from the dependence of the radius of gyration of the agglomerate, R_g , on the number of spheres in the cluster, k . The radius of gyration is related to the second moment of the mass distribution and is defined by

$$mR_g^2 = \sum_{i=1}^k m_i r_i^2, \quad (48)$$

where r_i is the distance from the center of mass of the agglomerate to the i th sphere and m is the total mass of the agglomerate.

In Fig. 2, R_g is plotted versus k for the case $\beta\tau = 0.05$ and density $\rho = 0.0167$. The quantity ρ is defined as the number of particles per volume

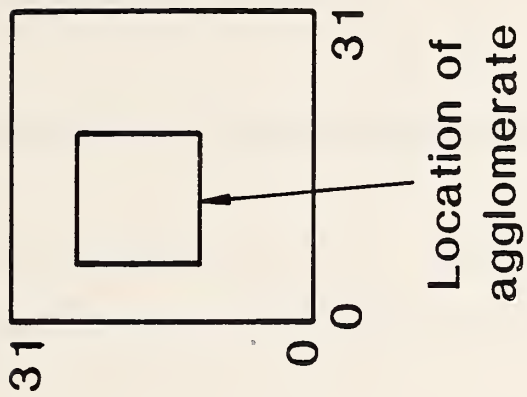
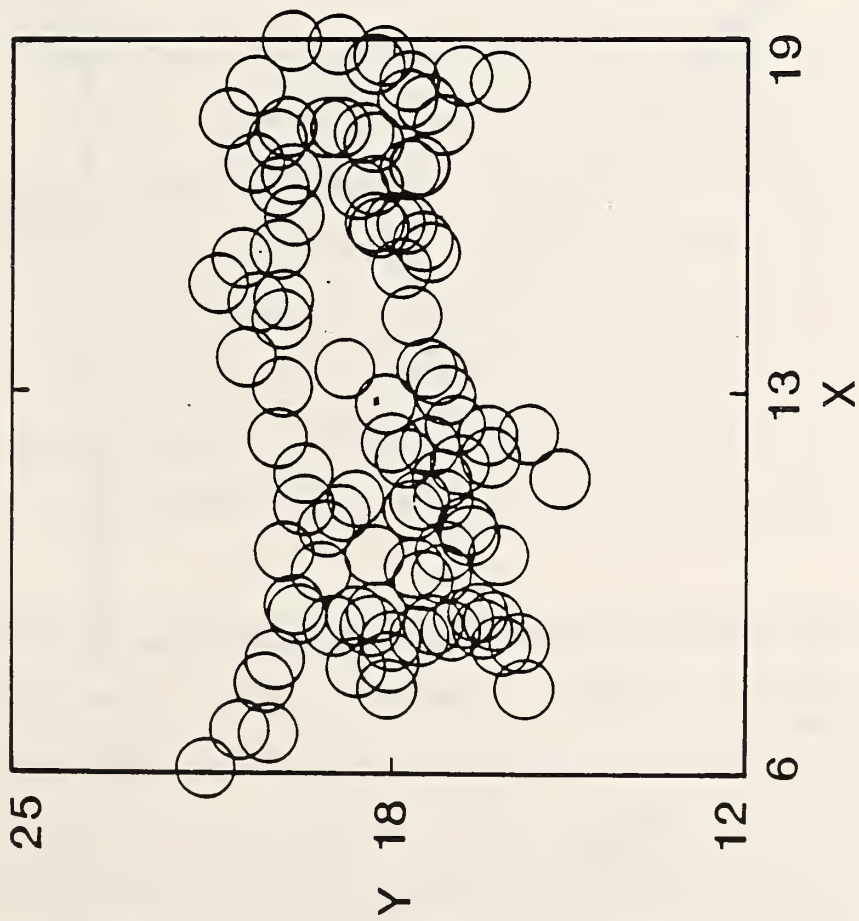


Figure 1. Planar projection of an agglomerate with 90 spheres is displayed for a simulation based on 500 spheres randomly distributed in a cube with edge length 31σ ($\beta\tau = 0.2$).

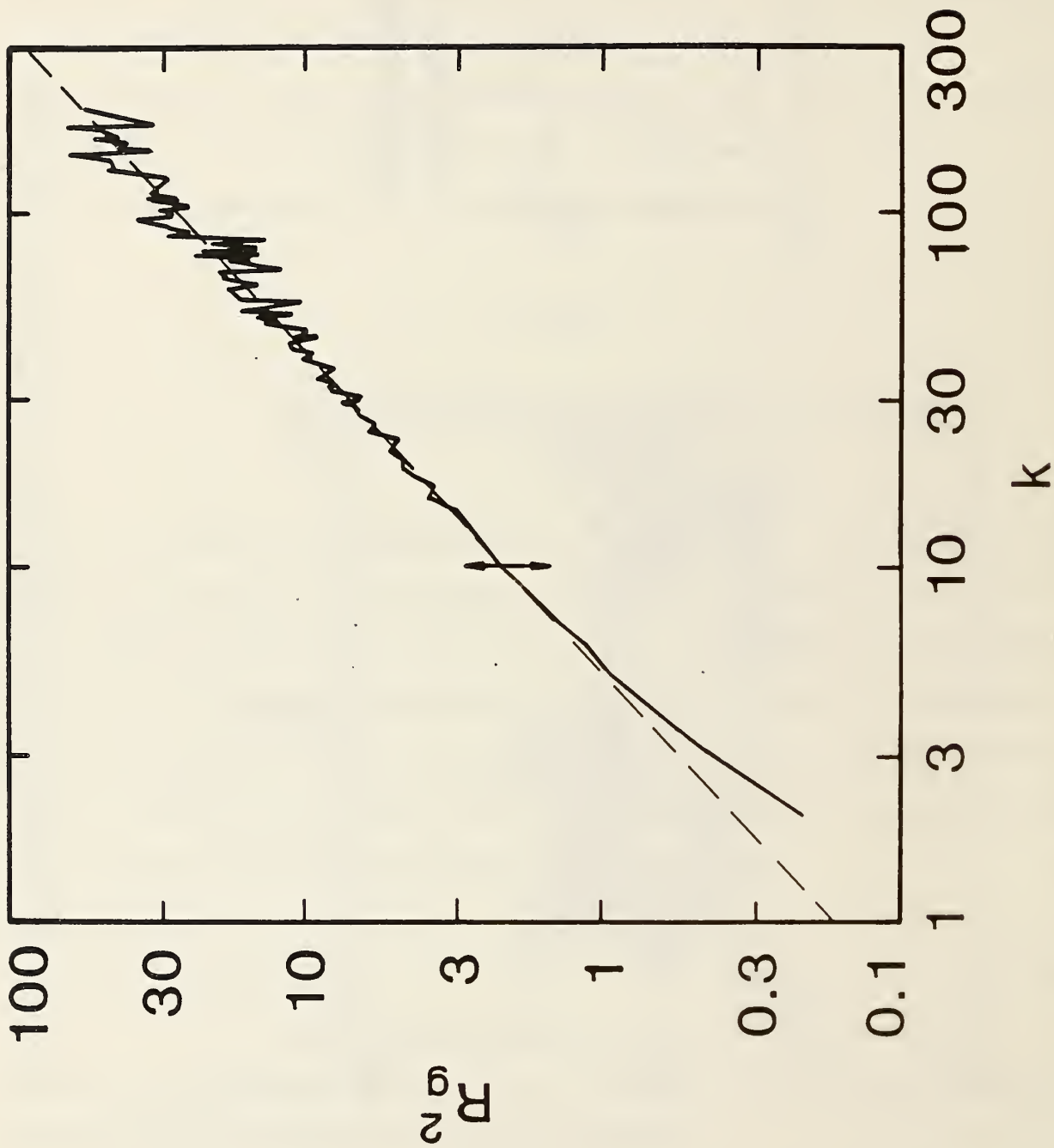


Figure 2. The square of the radius of gyration, R_g , in units of σ , is plotted versus the number of spheres in the agglomerate, k , for $\beta T = 0.05$ and $\rho = 0.0167$. The curve represents the average values of R_g and the pointer corresponds to one sigma. The dashed line corresponds to a fractal dimension of 1.80.

where volume is in units of σ^3 . Over the cluster size range from about 5 to 200, R_g has a power law dependence on k given by

$$R_g = Ak^\alpha \quad (49)$$

where $\alpha = 0.55$ and $A = .42$ for R_g in units of σ_g . This power law dependence is consistent with a fractal dimensionality D_α given by [24]

$$D_\alpha = 1/\alpha, \quad (50)$$

which in this case is 1.8. For a fixed k the sigma for R_g^2 is about 20 to 30% of the quantity itself. The large variability in R_g^2 for agglomerates greater than about 50 arises from the relative infrequency of any one large agglomerate out of ten repeat simulations. We have also performed simulations for $\beta\tau = 0.2$ and for $\rho = 0.05, 0.0167, \text{ and } 0.005$. In all cases the dimensionality inferred from the plots is in the range 1.7-1.9. Our results for D_α are in good agreement with Meakin's results [3] for D_α (1.75) based on the dependence of R_g on k for Brownian trajectories of clusters on a lattice.

We find that over the agglomerate size range accessible to our simulations, 5 to 200, the fractal dimension in the continuum fluid mechanical regime is essentially identical with the results found in the free molecular simulations. Meakin [25] arrived at a similar conclusion that the size dependence of the agglomerate diffusion coefficient did not affect the fractal dimension based on Monte Carlo simulations in two dimensions. The data for the longest run in the continuum flow regime are given in Fig. 3, which corresponds to $\rho = 0.0167$. This fit of the data yields

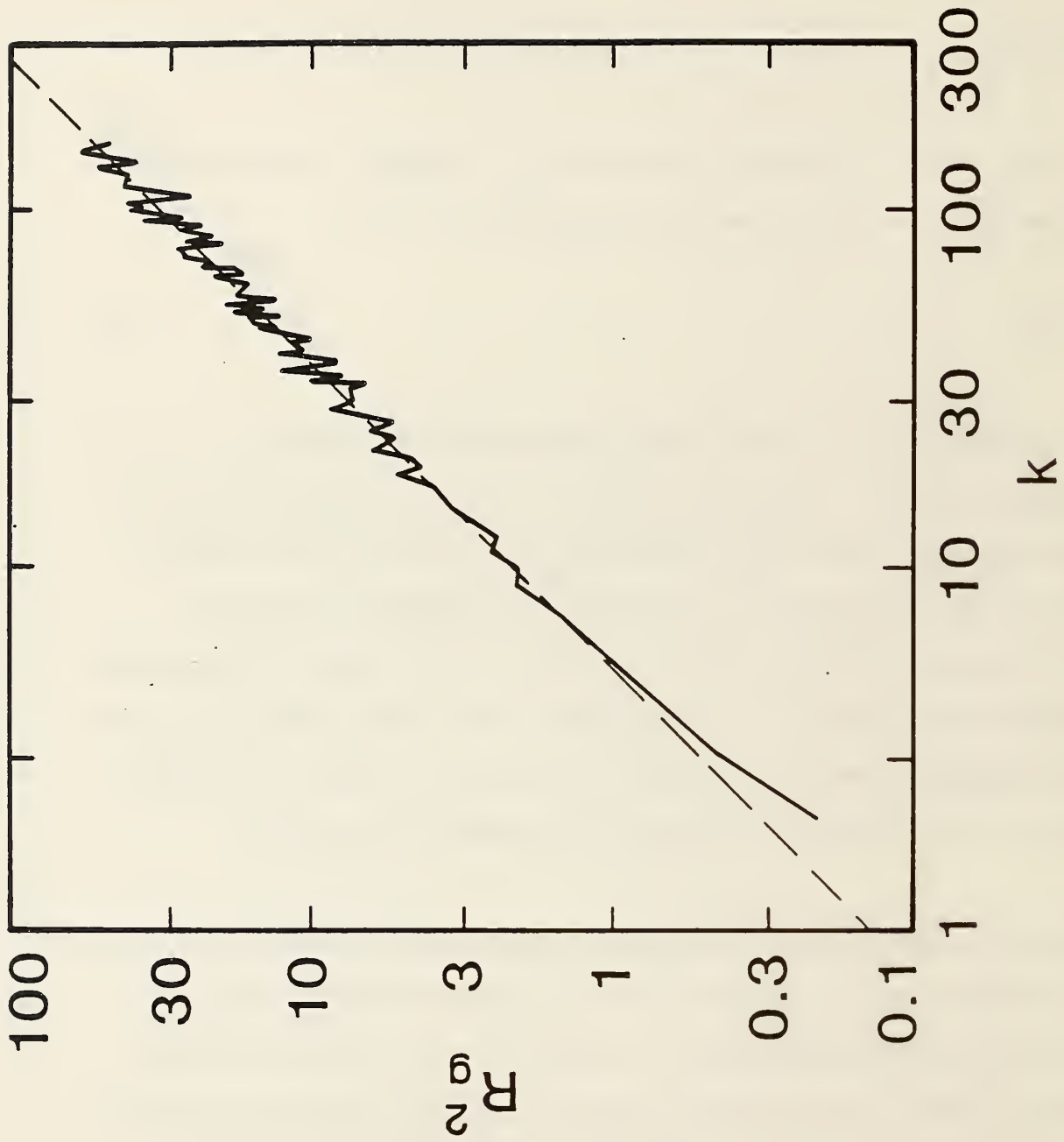


Figure 3. K_G^2 vs k for continuum flow for $\rho = 0.0167$ with the dashed line corresponding to a fractal dimension of 1.70.

$$R_g = 0.38 k^{0.59} \quad (51)$$

with a fractal exponent of 1.7.

4.2 Kinetics

A major interest in our study is the kinetics of cluster agglomeration.

A global measure of the kinetics is the time dependence of the total number of clusters, N , defined by

$$N = \sum_k n_k. \quad (52)$$

The quantity $\frac{N_0}{N(t)} - 1$ is convenient for displaying the results of the simulations. First, coagulation theory for a constant coagulation coefficient predicts that this reduced number concentration is proportional to the product of the initial number concentration and time. Secondly, the reduced number concentration is simply related to the change in the average particle volume \bar{v} .

$$\frac{N_0}{N(t)} - 1 = \frac{\bar{v}(t) - \bar{v}_0}{\bar{v}_0} \quad (53)$$

The results of the free molecular simulation for both $\beta\tau = 0.05$ and 0.2 are contained in Fig. 4. As the concentration decreases from 0.05 to 0.0167 to 0.005 , more time is required for agglomeration to take place. In all cases we see that the slope increases with time from a value of about 1 at early time to a value greater than 2 at the time when the total number of cluster has decreased by a factor of about 20. Provided $\beta\tau$ is small enough so that

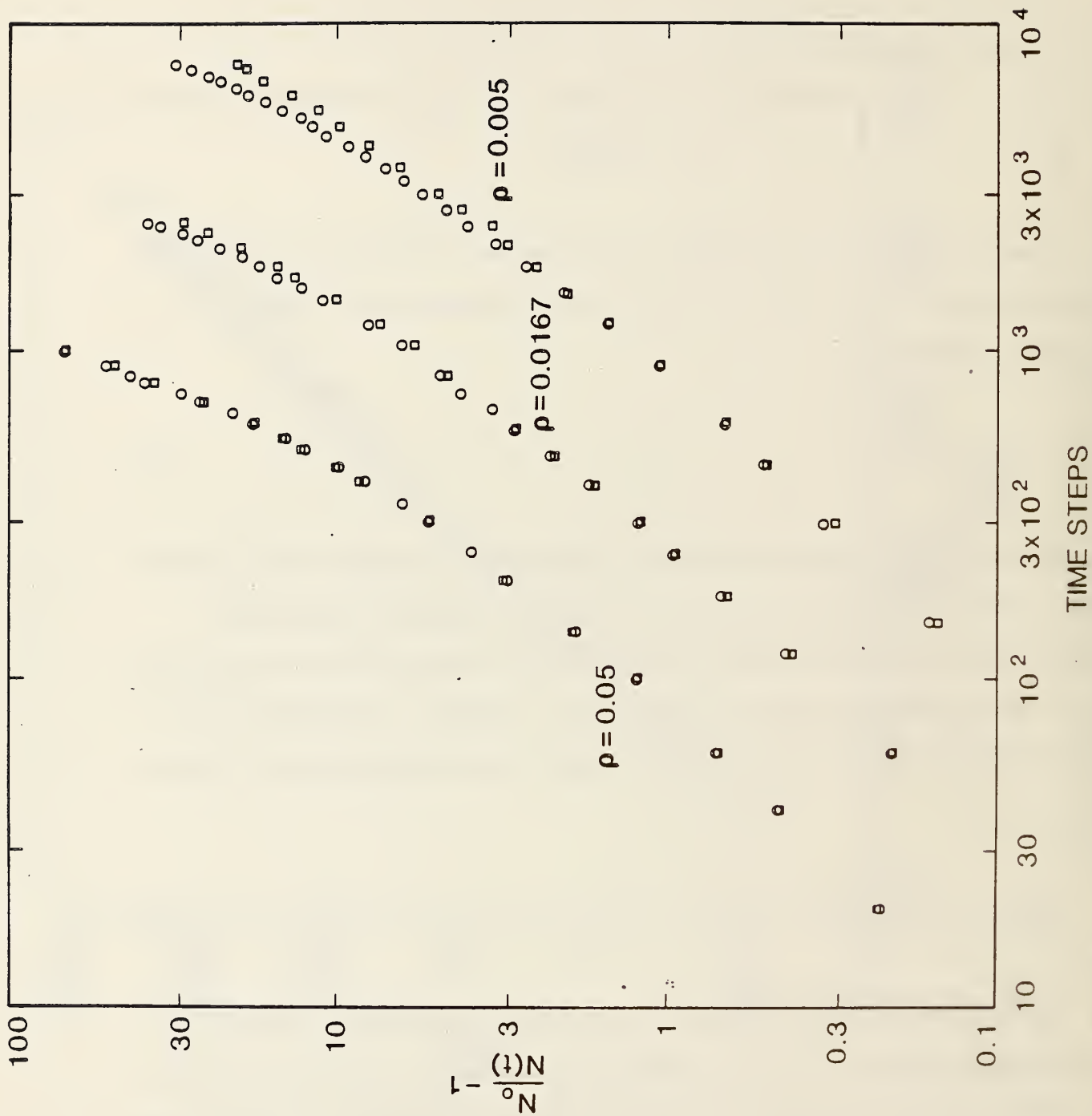


Figure 4. Reduced number concentration versus time steps for free molecular flow ($\beta I = 0.05$ ○, $\beta I = 0.2$ □) at three concentrations, $\rho = 0.05$, 0.0167 , and 0.005 .

the free molecular limit applies, the kinetics should be insensitive to the value of $\beta\tau$. The fact that the results for $\beta\tau = 0.2$ lie slightly below the results for $\beta\tau = 0.05$ suggests that the agglomerate trajectory is not quite free molecular in this case. The condition for free molecular behavior depends not only on the size of the individual sphere but also on the size of the agglomerate.

In an attempt to correlate the kinetic data, we plot the data versus a reduced time, t_N , in Fig. 5

$$t_N = (\text{time steps}) (\rho) \quad (54)$$

As pointed out above, coagulation theory for constant coagulation coefficient predicts that the reduced number concentration, $\frac{N_0}{N(t)} - 1$, is proportional to the product of the initial number concentration times time. We see that all of the data are reduced to one curve. For long time the slope increases to about 2.6, though because of the limited data it is not certain that an asymptotic power law behavior has been reached.

The kinetics of the agglomeration process is considerably different in the continuum regime. The slope increases only slightly with time up to a value of about 1.15 compared to 2.6 in the free molecular regime. The use of the reduced time variable t_N does not collapse all of the data to one curve (see Fig. 6) as was the case for the free molecular simulations. Also, as shown in Fig. 6, the small time behavior for the simulations seems to diverge from the coagulation theory prediction instead of converging to it. This is surprising since one would expect coagulation theory to be valid at small time

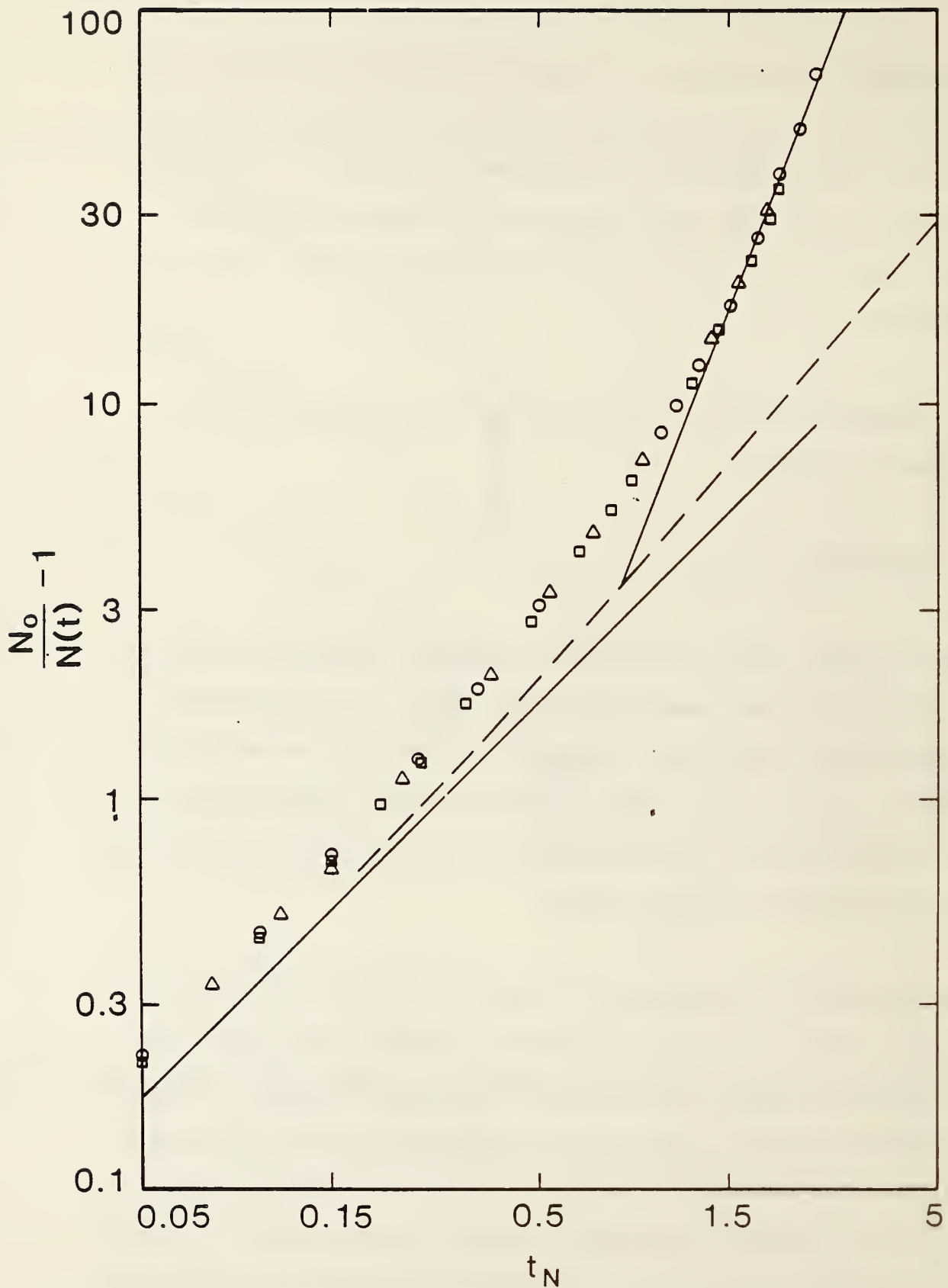


Figure 5. Reduced number concentration versus reduced time (time steps $\times \rho$) for $\beta\tau = 0.05$ and $\rho = 0.05$ (o), $\rho = 0.0167$ (\square), and $\rho = 0.005$ (Δ). The dashed line corresponds to the calculation of Lai *et al.* and the solid line to coagulation theory for constant coagulation.

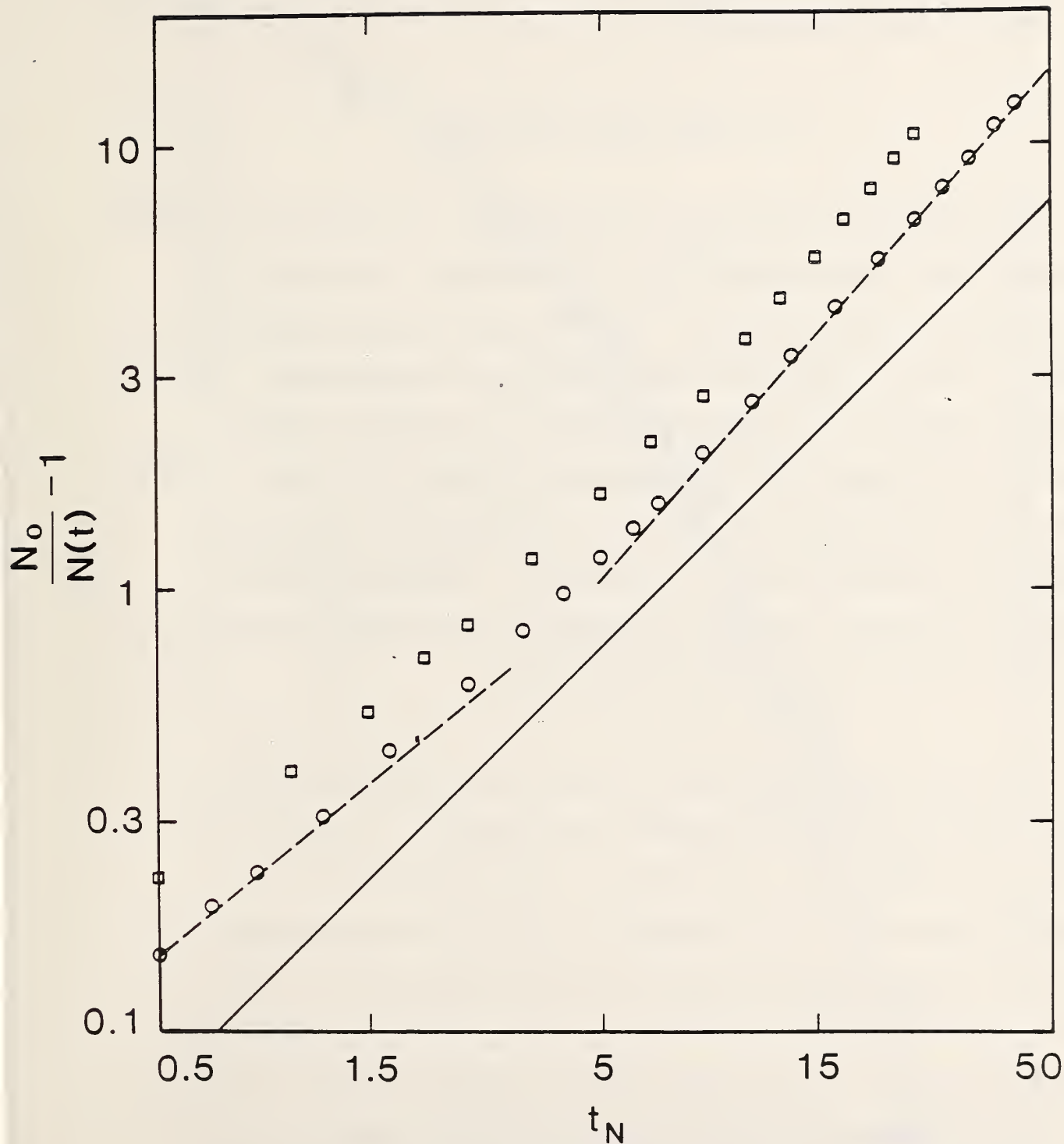


Figure 6. Reduced number concentration versus t_N for continuum flow with $\rho = 0.05$ (\square) and $\rho = 0.0167$ (\circ). The solid line corresponds to the prediction based on the coagulation theory and the dashed lines to the slopes for long time (1.15) and short time (0.85).

when there are relatively few agglomerates. In the next section an explanation for this result will be given.

4.3 Cluster Size Distribution

The information on the cluster size distribution is limited by the relatively small number of particles in the simulation. The cluster size distributions are plotted in Figs. 7 and 8 for times corresponding to approximately a 5 fold and 9 fold drop in the initial number concentration. The free molecular solution of the coagulation equation for coalescing droplets obtained by Lai et al. [26] is consistent with the data. Even the Smoluchowski solution [27] for the case of size independent coagulation coefficient is within the scatter of the "data". The major qualitative conclusion is that the cluster size distribution is more nearly exponential in character than power law for large cluster sizes.

The cluster size distributions for the continuum regime are plotted in Figs. 9 and 10 for times corresponding to approximately a 3 fold and 9 fold drop in the initial number concentration. The continuum solution of the coagulation equation obtained by Hidy [28], as well as the Smoluchowski solution [27], are in reasonable agreement with the simulations. So, while there is no a priori reason to expect agreement between the cluster agglomeration simulations and the solution of the coagulation equation, we do in fact see agreement within the uncertainty of the simulations for clusters of size 30 and less. We must await much larger simulations to better define the cluster size distribution especially in the large agglomerate region.

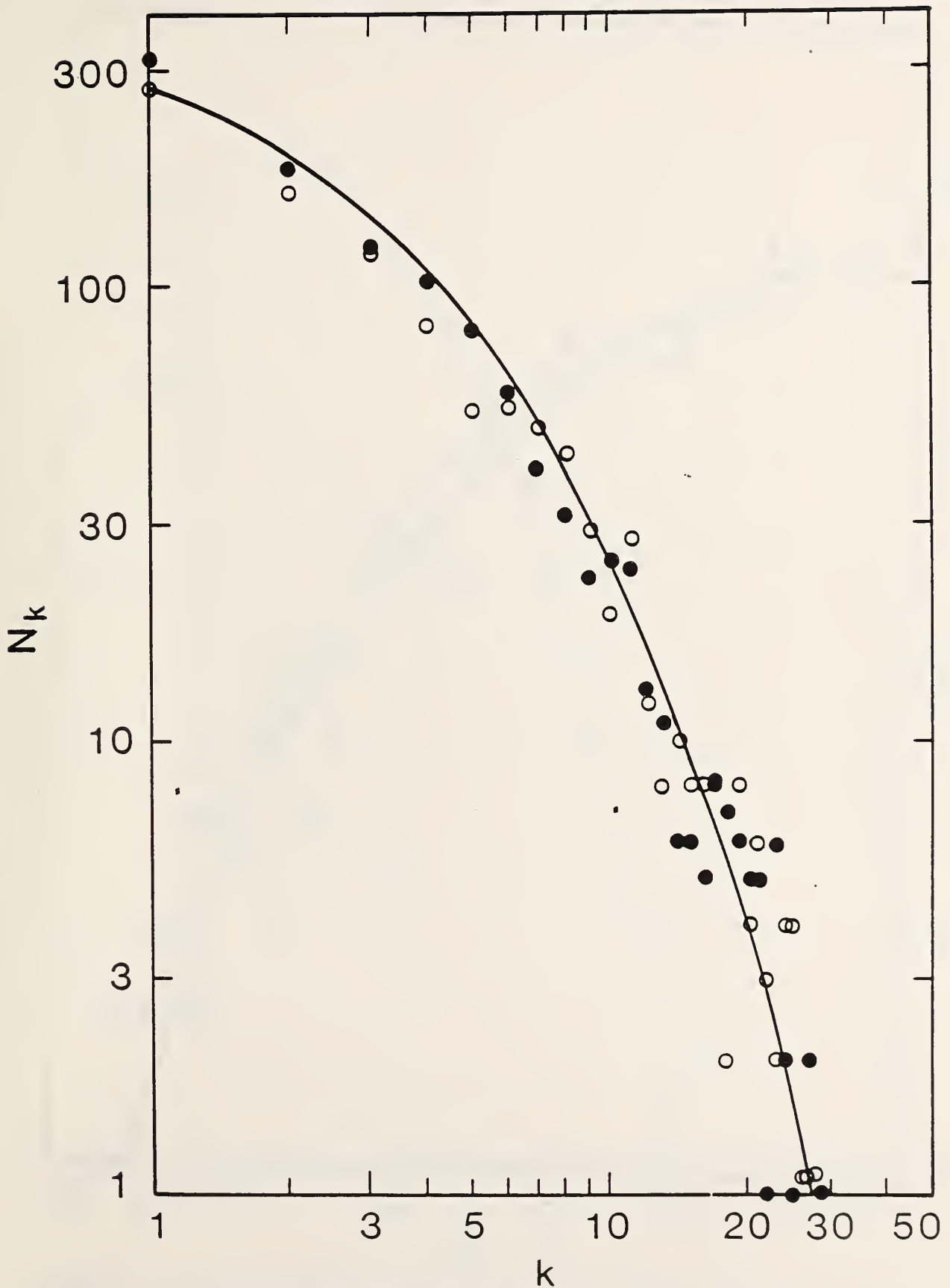


Figure 7. The cluster size distribution is plotted for free molecular simulation ($\beta\tau = 0.2$, $\rho = 0.05$ [O] and $\beta\tau = 0.05$, $\rho = 0.05$ [•]) for $N_0/N(t) = 4.5$. The solid curve corresponds to the solution of the coagulation equation by Lai et al.

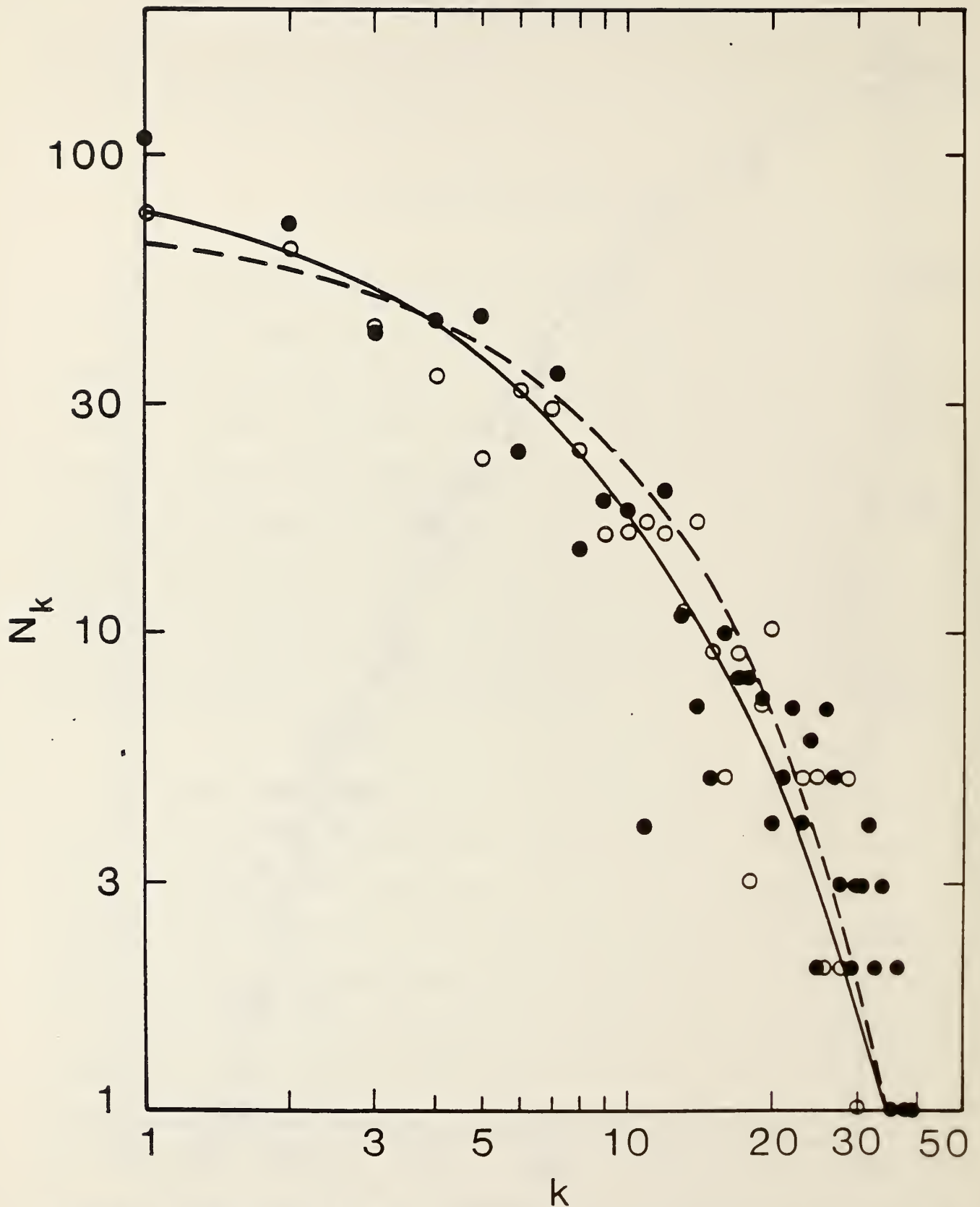


Figure 8. The cluster size distribution is plotted for $N_0/N(t) = 8.7$ for the same simulations as Fig. 7. The solid line corresponds to the Lai *et al.* solution and the dashed curve to the Smoluchowski solution to the coagulation equation.

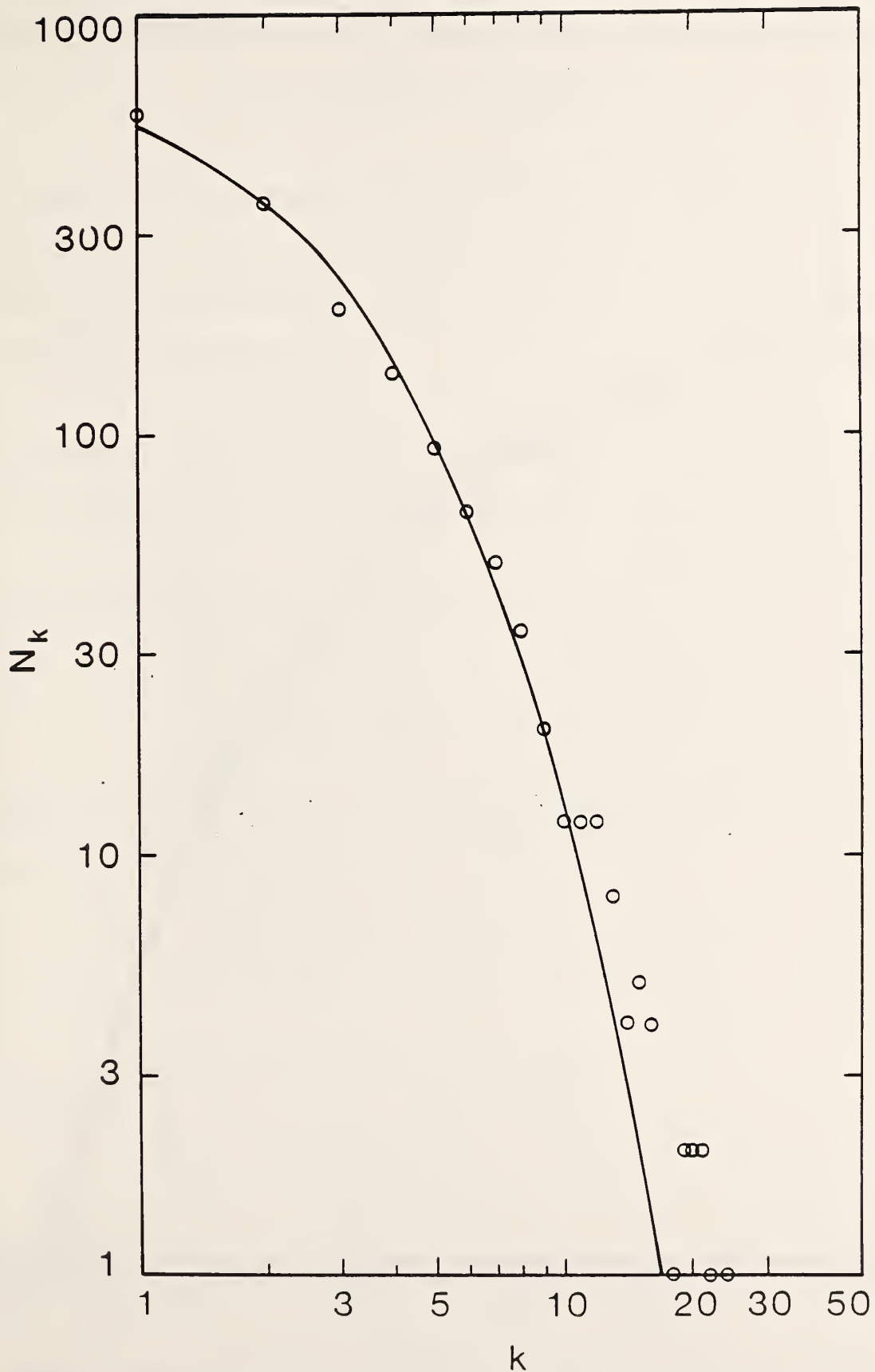


Figure 9. The cluster size distribution is plotted for the continuum simulation ($\rho = 0.0167$) for $N_0/N(t) = 3$. The solid line corresponds to the Hidy solution for the coagulation equation.

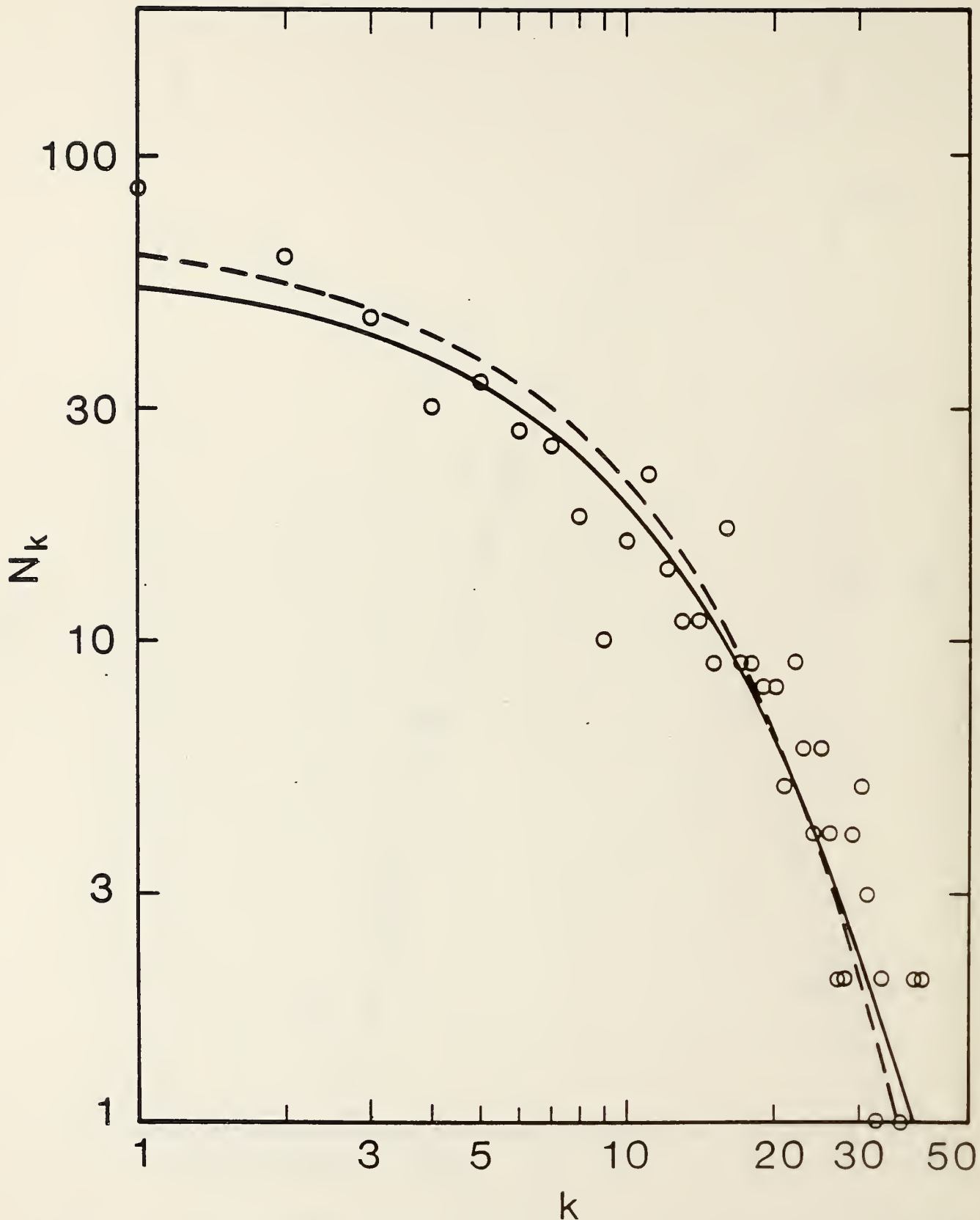


Figure 10. The cluster size distribution is plotted for $N_0/N(t) = 9$ for the same simulation as Fig. 9. The solid and dashed lines correspond to the Hidy and Smoluchowski solutions of the coagulation equation, respectively.

5. COAGULATION EQUATION

In this section, we present the results of coagulation theory for comparison with the simulations. We also use a similarity transform of the coagulation equation to determine the long time kinetics for an "agglomeration" type coagulation coefficient.

The evolution of the size distribution function $n(v,t)$ for coalescing droplets of volume v is described by the coagulation equation:

$$\begin{aligned} \partial n(v,t)/\partial t = & \frac{1}{2} \int_0^v K(v', v-v') n(v', t) n(v-v', t) dv' \\ & - n(v, t) \int_0^\infty K(v, v') n(v', t) dv' \end{aligned} \quad (55)$$

The coagulation coefficient $K(v, v')$ for the free molecular (fm) and continuum (c) regime are given by

$$K(v, v') = \left(\frac{3}{4\pi}\right)^{1/6} \left(\frac{6k_B T}{\rho_s}\right)^{1/2} (v^{1/3} + v'^{1/3})^2 \left(\frac{1}{v} + \frac{1}{v'}\right)^{1/2} \quad \text{fm} \quad (56)$$

$$\begin{aligned} K(v, v') &= \frac{2k_B T}{3\eta} (v^{1/3} + v'^{1/3}) \left(\frac{1}{v^{1/3}} + \frac{1}{v'^{1/3}}\right) \\ &= \frac{2k_B T}{3\eta} (r + r') \left(\frac{1}{r} + \frac{1}{r'}\right), \end{aligned} \quad \text{c} \quad (57)$$

were r and r' are the radii of spheres with volume v and v' , respectively.

For small time, most of the particles are individual spheres so that treating K as a constant in eq. (55) is a good approximation. Integrating

both sides of eq. (55) over all particle sizes and solving the resulting ordinary differential equation for $N(t)$, we obtain

$$N(t)/N_0 = (1 + \frac{1}{2} K N_0 t)^{-1}. \quad (58)$$

The expressions for K in the two limits are obtained by setting $v = v'$.

$$K = 4 \sqrt{2} \left(\frac{6rk_B T}{\rho_s} \right)^{1/2} \quad \text{fm} \quad (59)$$

$$K = \frac{8 k_B T}{3\eta} \quad \text{c} \quad (60)$$

It is convenient for comparison with the simulations to express eq. (58) in the following form:

$$N_0/N(\tau_1) - 1 = \frac{1}{2} K \frac{\tau}{\sigma^3} \tau_1, \quad (61)$$

where $\tau_1 = (t/\tau) \rho$. In the two limits, we obtain

$$N_0/N(\tau_1) - 1 = 2 \sqrt{\pi} \tau_1 \quad \text{fm} \quad (62)$$

$$N_0/N(\tau_1) - 1 = \frac{4\pi\tau_1}{\beta\tau} \quad \text{c} \quad (63)$$

In the free molecular limit, the simulation results at small time for the reduced number concentration are about 20% greater than predicted by eq. (62) (see Fig. 5). This increase may result from fluctuations arising in the simulation which are not taken into account in the coagulation equation. We have also performed simulations without agglomeration in which a pair of

colliding particles is replaced with a single particle of mass m_0 to eliminate any size dependence of the coagulation process. We still obtain slightly more rapid growth compared to the prediction of the coagulation equation with constant K .

As pointed out in the previous section, the simulation and the prediction based on the coagulation equation for the continuum regime seem to be diverging rather than converging at small time (Fig. 6). Also the results of the simulation depend on ρ while the solution of the coagulation equation is independent of ρ . The cause of the discrepancy is a small-time enhancement in the coagulation rate for very high particle concentration [29,30]. The derivation of eq. (60) involves the calculation of the rate at which particles arrive at the surface of a sphere, $F(t)$. For equal size spheres of diameter σ , the solution of the diffusion equation with absorbing boundary conditions [31] is given by

$$F(t) = 4\pi D\sigma n_\infty \left(1 + \frac{\sigma}{(\pi Dt)^{1/2}} \right), \quad (64)$$

where D is the particle diffusion coefficient. The transient term is dropped in deriving eq. (60); however, this approximation is not valid at small times. For example, for $t_N = 1.66$, which corresponds to 0.05 s for $\rho = 0.0167$ and 0.0167 s for $\rho = 0.05$, we obtain sizeable transient terms for a 1 μm diameter sphere in air

$$\frac{\sigma}{(\pi Dt)^{1/2}} = 0.52 \quad \rho = 0.0167$$

$$\frac{\sigma}{(\pi Dt)^{1/2}} = 0.90 \quad \rho = 0.05$$

This transient effect is the major cause for the difference in the small time behavior for the simulation and the coagulation equation. At lower concentrations the effect is less pronounced since the time required for coagulation is longer. For aerosols, ρ would seldom be greater than 10^{-6} , and under these conditions the transient term is negligible. We are not able to simulate such dilute conditions because of the long computation time required. As an aside, values of ρ as large as 10^{-1} exist in colloidal systems, so in this case deviations of the sort seen in Fig. 6 are to be expected.

We next consider the solution of the coagulation equation for an "agglomerate" coagulation coefficient to compare with the results of the simulation. Assuming $K(v, v')$ to be symmetric, it can be shown that

$$\frac{dN}{dt} = \int_0^{\infty} \int_0^{\infty} K(v, v') n(v) n(v') dv dv'. \quad (65)$$

In the free molecular limit, the coagulation coefficient consists of a collision cross section term multiplying a velocity term. The cross section of a low density agglomerate will be much greater than a compact sphere. The expression for the coagulation coefficient, eq. (56), is modified to apply to an agglomerate by replacing the $v^{1/3}$ term, which is related to the collision cross section, with the radius of gyration, R_g . We then make use of the fractal character of the agglomerate, eq. (49), to express R_g in terms of $v^{1/D}$. So the v dependence of K for the agglomerate can be expressed as

$$K(v, v') \sim (v^{1/D} + v'^{1/D})^2 \left(\frac{1}{v} + \frac{1}{v'} \right)^{1/2}. \quad (66)$$

To solve for $N(t)$ it is convenient to use the similarity variables ψ , the dimensionless size distribution function, and v , the dimensionless particle volume.

$$\psi = \frac{n(v,t)}{N(t)^2} V \quad (67)$$

$$v = \frac{vN(t)}{V} \quad (68)$$

The volume concentration V is conserved during particle coagulation.

Substituting eq. (66) into eq. (65) and expressing n and v in terms of ψ and v , we obtain

$$\frac{dN}{dt} \sim N^{\frac{5}{2} - \frac{2}{D} - \frac{2}{vD} - \frac{1}{2}} A. \quad (69)$$

The quantity A includes dimensionless integrals involving various moments of $\psi(v)$. Integrating eq. (69), we obtain

$$\frac{N_0}{N(t)} \sim t^p, \quad (70)$$

$$\text{where } p = \left(\frac{3}{2} - \frac{2}{D}\right)^{-1}. \quad (71)$$

For $D = 1.80$, we obtain $p = 2.57$ which is in good agreement with the simulation result of 2.6. The value of p is very sensitive to the fractal exponent. For D set equal to 3, we recover the free molecular solution of Lai et al. [26], $p = 6/5$.

Next we consider the continuum limit. In eq. (57) the first term involving radius relates to the collision radius, whereas the second relates to the diffusion coefficient. For the case of an agglomerate, we replace both radii with the radius of gyration but for different reasons. In the first case it is because the characteristic collision radius of an agglomerate is R_g . In the second case the diffusion coefficient of an agglomerate is inversely proportional to the friction force, which is proportional to R_g for an agglomerate. Using the relationship between R_g and v , we obtain

$$K(v, v') \sim (v^{1/D} + v'^{1/D}) \left(\frac{1}{v^{1/D}} + \frac{1}{v'^{1/D}} \right) \quad (72)$$

Carrying out the same type of analysis as in the free molecular case, we obtain

$$\frac{N_0}{N(\tau)} \sim \tau. \quad (73)$$

In this case the time dependence is the same as for a compact structure. The enhancement arising from the increased collision radius is cancelled out by the decrease in the diffusion coefficient. The simulation yields a slightly stronger time dependence, $\tau^{1.15}$, than that predicted by coagulation theory. This may be an artifact of the high initial concentration, for which the coagulation equation is not valid, or that the simulation was not carried to long enough time.

The analysis of the coagulation equation given above is intuitive. To be rigorous one must verify that the similarity solution exists. Van Dongen and Ernst [32] have derived a generalized scaling form for the size distribution function. They find

$$\frac{N_0}{N(\tau)} \sim \tau^Z, \quad (74)$$

where $Z = \frac{1}{1 - \lambda}$.

The quantity λ is determined by the scaling characteristics of the coagulation coefficient.

$$k(av, av') = a^\lambda k(v, v') \quad (75)$$

The results of Van Dongen and Ernst are identical with our results for K given by eqs. (66) and (72).

6. COMPARISON WITH EXPERIMENTS

Forrest and Witten [33] have obtained fractal dimensions in the range of 1.5 to 1.7 for inorganic smokes, including Fe and Zn. The smokes were produced by rapidly heating a tungsten wire plated with metal. The fractal dimension was determined from the power law dependence of the density autocorrelation function.

Feder et al. [34] have inferred from Medalia and Heckmans' measurements on carbon black [35] a fractal dimension of 2.3. The difference from the inorganic smoke may arise from the ultrasonic dispersion of the collected carbon black particles in a liquid. The dispersion process apparently breaks weak bonds in the agglomerates resulting in smaller, perhaps, more compact structures. The present computer simulations are in fair agreement with the inorganic smoke but are apparently less compact than carbon black.

There are very little data on the kinetics of agglomeration in the gas phase. Howard et al. [36] have measured the coagulation rate of carbon particles in a low pressure, premixed flame. The primary particle size is about 10 nm and the pressure about 20 Torr. This corresponds to free molecular behavior with $\beta\tau \approx 0.002$. The experimentally observed coagulation rate was found by Howard et al. to exceed by a factor of 10 the free molecular coagulation rate approximately adjusted for electrostatic forces and Van der Waals attraction. The number concentration decreased by a factor of six with increasing height in the flame. The results of the free molecular simulation shown in Fig. 5 suggest that as the total number concentration decreases by a factor of six the agglomeration kinetics will approximately double the growth rate compared to the solution of the coagulation equation. The electron micrographs clearly show the formation of agglomerates. However, agglomeration by itself will not account for the entire factor of 10 difference between the theoretical and experimental result. It is also possible that the measured absolute number concentration was systematically underestimated by the electron microscopy. Even under the best of circumstances, a measurement of the absolute number concentration of an aerosol is difficult.

7. ACKNOWLEDGMENT

The authors acknowledge support by Defense Nuclear Agency in carrying out this research. The authors also acknowledge Francis Sullivan for his assistance in developing an efficient computer code.

8. REFERENCES

- [1] Phalen, R.F., *Aerosol Sci* 5, 465 (1974).
- [2] Sutherland, D.N., *J. Colloid and Interface Sci.* 25, 373 (1967).
- [3] Meakin, P., *Phys. Rev. A.* 29, 997 (1984).
- [4] Kolb, M., Botet, R., and Jullien, R., *Phys. Rev. Lett.* 51, 1123 (1983).
- [5] Vold, M.J., *J. Colloid Sci.* 18, 684 (1963).
- [6] Witten, T.A., Jr. and Sander, L.M., *Phys. Rev. Lett.* 47, 1400 (1981);
Witten, T.A. and Sander, L.M., *Phys. Rev.* B27, 5686 (1983).
- [7] Richter, R., Sander, L.M., and Cheng, Z., *J. Colloid and Interface Sci.* 100, 203 (1984).
- [8] Sullivan, F. and Mountain, R.D., submitted to *Computer Physics Communication*.
- [9] Meakin, P., Chen, Z.Y., and Deutch, J.M., *J. Chem. Phys.* 82, 3786 (1985).
- [10] Ermack, D.L. and Buckholtz, H., *J. Comp. Phys.* 35, 169 (1980).
- [11] Chandrasekhar, S., *Rev. Mod. Phys.* 15, 1 (1943).
- [12] Mountain, R.D., *Phys. Rev.* A26, 2859 (1982).
- [13] Sullivan, F., Mountain, R.D. and O'Connell, J., *J. Comput. Phys.* (in press).
- [14] Meakin, P., *J. Chem. Phys.* 81, 4637 (1984).
- [15] Epstein, P.S., *Phys. Rev.* 23, 710 (1924).
- [16] Proudman, I. and Pearson, J.R.A., *J. Fluid Mech.* 2, 237 (1957).
- [17] Van Dyke, M., *Perturbation Methods in Fluid Mechanics*, Academic Press, New York, 153 (1964).
- [18] Felderhof, B.U., *Physica* 80A, 63 (1975).
- [19] Lamb, H., *Hydrodynamics*, Dover, New York, p. 610 (1932).
- [20] Felderhof, B.U. and Deutch, J.M., *J. Chem. Phys.* 62, 2391 (1975).
- [21] Overbeck, H.A., *Journal für die reine und angewandte Mathematik* 81, 62 (1876).
- [22] Horvath, H., *Staub Reinhaltung der Luft* 34, 197 (1974).

- [23] Kirkwood, J.G. and Riseman, J., J. Chem. Phys. 16, 565 (1948).
- [24] Stanley, H.E., J. Phys. A 10, L 211 (1977).
- [25] Meakin, P., Phys. Rev. B29, 2930 (1984).
- [26] Lai, F.S., Friedlander, S.K., Pich, J., and Hidy, G.M.J., Colloid Interface Sci. 39, 395 (1972).
- [27] Smoluchowski, M., Z. Physik Chem. 92, 129 (1917a).
- [28] Hidy, G.M., J. Colloid and Interface Sci. 20, 123 (1965).
- [29] Ziff, R.M., McGrady, E.D., and Meakin, P., J. Chem. Phys. 82, 5269 (1985).
- [30] Mulholland, G.W. and Mountain, R.D., accepted for publication in J. Chem. Phys.
- [31] Friedlander, J.K., Smoke, Dust and Haze, Wiley and Sons, New York (1977).
- [32] Van Dongen, P.G.J. and Ernst, M.H., Phys. Rev. Lett. 54, 1369 (1985).
- [33] Forrest, S.R. and Witten, T.A., Jr., J. Phys. A. 12, L109 (1979).
- [34] Feder, J., Jossang, T. and Rosengvist, E., Phys. Rev. Lett. 53, 1403 (1984).
- [35] Medalia, A.I. and Heckman, F.A., J. Colloid and Interface Sci. 36, 173 (1971).
- [36] Howard, J.B., Wersborg, B.L., and Williams, G.C., Faraday Symposia of the Chemical Society No. 7, Fogs and Smokes, 109 (1973).

U.S. DEPT. OF COMM. BIBLIOGRAPHIC DATA SHEET <i>(See instructions)</i>	1. PUBLICATION OR REPORT NO. NBSIR 86-3342	2. Performing Organ. Report No.	3. Publication Date March 1986
4. TITLE AND SUBTITLE Simulation of Aerosol Agglomeration in the Free Molecular and Continuum Flow Regimes			
5. AUTHOR(S) George W. Mulholland, Raymond D. Mountain, and Howard Baum			
6. PERFORMING ORGANIZATION <i>(If joint or other than NBS, see instructions)</i> NATIONAL BUREAU OF STANDARDS DEPARTMENT OF COMMERCE WASHINGTON, D.C. 20234		7. Contract/Grant No.	8. Type of Report & Period Covered
9. SPONSORING ORGANIZATION NAME AND COMPLETE ADDRESS <i>(Street, City, State, ZIP)</i> Defense Nuclear Agency Washington, DC 20305			
10. SUPPLEMENTARY NOTES <input type="checkbox"/> Document describes a computer program; SF-185, FIPS Software Summary, is attached.			
11. ABSTRACT <i>(A 200-word or less factual summary of most significant information. If document includes a significant bibliography or literature survey, mention it here)</i> The formation of high temperature aerosol agglomerates is simulated by following the Langevin trajectory of each particle with the boundary condition that the particles stick upon collision. Both the free molecular and continuum flow are treated. A new derivation of the friction force of an agglomerate in the continuum limit is developed based on the evaluation of the surface momentum flux at the Oseen flow limit. The agglomerates can be described as fractal, at least in regard to power law relationship between mass and size, with a dimensionality of 1.7-1.9 independent of the flow regime. The particle growth is shown to be much more rapid in the free molecular regime than in the continuum. The global kinetics are shown to be consistent with a similarity analysis of the coagulation equation with a modified coagulation coefficient. Comparison between the simulation and coagulation theory at small time suggests a slight fluctuation enhancement in the free molecule case and a small-time enhancement of the coagulation rate at high concentration for the continuum case.			
12. KEY WORDS <i>(Six to twelve entries; alphabetical order; capitalize only proper names; and separate key words by semicolons)</i> aerosol agglomeration; agglomerates; Brownian motion; Darcy's law; fractal dimensions; free molecular regime; Smoluchowski equation; soot			
13. AVAILABILITY <input checked="" type="checkbox"/> Unlimited <input type="checkbox"/> For Official Distribution. Do Not Release to NTIS <input type="checkbox"/> Order From Superintendent of Documents, U.S. Government Printing Office, Washington, D.C. 20402. <input checked="" type="checkbox"/> Order From National Technical Information Service (NTIS), Springfield, VA. 22161		14. NO. OF PRINTED PAGES 49	15. Price \$9.95

